

Optical Engineering

OpticalEngineering.SPIEDigitalLibrary.org

Assembly process and optical performances for a golden laser spark-plug device

Pol Ribes-Pleguezuelo
Nicolaie Pavel
Erik Beckert
Christoph Damm
Axel Bodemann
Oana-Valeria Grigore
Gabriela Croitoru
Catalina-Alice Brandus
Nicolae-Tiberius Vasile
Ramona Eberhardt
Andreas Tünnermann

SPIE.

Pol Ribes-Pleguezuelo, Nicolaie Pavel, Erik Beckert, Christoph Damm, Axel Bodemann, Oana-Valeria Grigore, Gabriela Croitoru, Catalina-Alice Brandus, Nicolae-Tiberius Vasile, Ramona Eberhardt, Andreas Tünnermann, "Assembly process and optical performances for a golden laser spark-plug device," *Opt. Eng.* **58**(6), 065101 (2019), doi: 10.1117/1.OE.58.6.065101.

Assembly process and optical performances for a golden laser spark-plug device

Pol Ribes-Pleguezuelo,^{a,*} Nicolae Pavel,^b Erik Beckert,^a Christoph Damm,^a Axel Bodemann,^a Oana-Valeria Grigore,^b Gabriela Croitoru,^b Catalina-Alice Brandus,^b Nicolae-Tiberius Vasile,^b Ramona Eberhardt,^a and Andreas Tünnermann^a

^aFraunhofer Institute for Applied Optics and Precision Engineering IOF, Jena, Germany

^bNational Institute for Laser, Plasma and Radiation Physics, Laboratory of Solid-State Quantum Electronics, Magurele, Romania

Abstract. The low-stress Solderjet Bumping technique was employed to assemble the optical components of an increased-robustness laser spark-plug ignition device using the low melting alloys 96.5Sn3Ag0.5Cu and 80Au20Sn. A finite-element-method analysis, optical simulations, and a soldering parametrization test were performed to prove that different optical materials (sapphire, ECO-550, D-ZLaF52LA, TAC4, and N-SF11 glasses) could be fastened to the stainless steel body. The assembled spark-plug device featured a passively Q-switched Nd:YAG/Cr⁴⁺:YAG composite ceramic medium and delivered laser pulses with energy variable between 2.40 and 4.70 mJ, with 0.8 ns duration, suitable for inducing air breakdown phenomenon and engine combustion. © The Authors. Published by SPIE under a Creative Commons Attribution 4.0 Unported License. Distribution or reproduction of this work in whole or in part requires full attribution of the original publication, including its DOI. [DOI: 10.1117/1.OE.58.6.065101]

Keywords: laser ignition; spark plug; Solderjet Bumping; air breakdown; Nd:YAG/Cr⁴⁺:YAG; combustion.

Paper 190242 received Mar. 11, 2019; accepted for publication May 20, 2019; published online Jun. 13, 2019.

1 Introduction

Concern about the environment, which is degraded by hydrocarbon pollution and greenhouse gas emissions resulting from the ongoing use of internal combustion engines, requires the development of alternative techniques to power engines, or the investigation of methods that can improve the performances of current engines. It is obvious that the proven advantages of vehicles powered by electrical engines will trigger further developments in this field. On the other hand, it is also largely accepted that combustion will, for many years, remain the dominant conversion process providing energy for society. Therefore, improved ignition methods, such as high energy spark-plug ignition (capacitive discharge, continuous discharge, or high-frequency multicharge ignition), pulse-power ignition (repetitive pulse spark or transient plasma ignition), radio-frequency ignition (spark, corona or microwave plasma ignition), or laser ignition (LI) are being investigated in order to initiate faster, more robust, and more efficient combustion.

LI can bring several advantages in comparison with ignition performed by classical electrical spark plugs (ESP).¹⁻⁴ With LI, there is no quenching effect on the combustion flame kernel, the laser beam can be delivered at any position within the combustion chamber, ignition can be obtained simultaneously at different points inside the cylinder, or lean air-fuel mixtures can be fired. LI was first employed to operate an engine (a one-cylinder ASTM-CFR engine) in 1978, by Dale et al.⁵ A large CO₂ laser with pulses having an energy of 0.3 J and 50 ns duration at 10.6 μm was used for the experiments. Furthermore, a real, four-cylinder Ford Mondeo engine was run via LI at Liverpool University in 2008, by Mullet et al.⁶ Here, electro-optically Q-switched

Nd:YAG lasers with emission at 1.06 μm were employed. All these experiments were performed with commercial lasers that were positioned nearby the engine; typically, the laser beams were guided by mirrors and then focused inside the engine cylinder through a transparent window. The real-world implementation of LI, however, requires compact laser sources that can reliably work in adverse conditions of pressure, vibration, and temperature and which can be directly installed on an engine, similar to an ESP. This noncentral ignition source arrangement, with one laser on each engine cylinder and a pump source located further away, was introduced in 2005 by Weinrotter et al.⁷

A solution for realizing a compact laser-spark plug (LSP) device was proposed in 2007, by Kofler et al.⁸ The system incorporated an Nd:YAG laser crystal which was passively Q-switched by a Cr⁴⁺:YAG saturable absorber (SA). The laser was built from discrete elements; the Nd:YAG medium was pumped longitudinally by a fiber-coupled diode laser and delivered pulses of 1.06 μm with energy up to 6.0 mJ and with a 1.5-ns pulse duration. Side-pumping with diode-array lasers was another scheme employed in 2009 by Kroupa et al.,⁹ to realize a compact and robust passively Q-switched Nd:YAG – Cr⁴⁺:YAG laser with 25 mJ of energy per pulse and 3 ns duration, operating at a repetition rate of up to 150 Hz. This laser, called HiPoLas[®], also consisted of discrete elements. One of the first compact passively Q-switched lasers resembling an ESP was reported in 2010 by Tsunekane et al.¹⁰ The laser was again composed of distinct elements; a 1.1-at.% Nd:YAG crystal, a Cr⁴⁺:YAG SA with an initial transmission $T_0 = 0.30$, and an out-coupling mirror (OCM) of reflectivity $R = 0.50$, yielding pulses of 3-mJ energy and 1.2-ns duration. A composite Nd:YAG/Cr⁴⁺:YAG ceramic medium in a monolithic resonator design was used by the same research group to demonstrate, in 2011, the first LSP device with a multiple-beam output.¹¹ Based on the development of

*Address all correspondence to Pol Ribes-Pleguezuelo, E-mail: pol.ribes@iof.fraunhofer.de

such compact LSPs, LI was successfully applied to operate real automobiles in 2013 by Taira et al.¹² and in 2015-2017 by Pavel et al.^{13,14} LI devices were also used in natural gas engines.¹⁵

As expected, there is understandably little public information about the internal design of an LSP device. However, it is obvious that the placement of the optical components and their attachment to the spark-plug body must ensure operation under difficult conditions of pressure, vibration, and temperature. In their previous work, Pavel et al.¹³ employed an epoxy adhesive, with high shear and peel strength, to fix the optical components (i.e., lenses, the sapphire window, and the Nd:YAG/Cr⁴⁺:YAG ceramic medium). In this paper, we report on the realization of an LSP device in which the assembling of the optical components was performed using the low-stress Solderjet Bumping soldering technique.¹⁶ The adapted LI device, here using soft-solder inorganic alloys, in contrast to commonly used organic adhesives. It promises higher robustness^{17,18} and assures space-compatible devices¹⁸ while avoiding damage to the optical components.^{19,20} The LSP optical design was performed to obtain a device that can induce air breakdown at a distance comparable to the electrical discharge distance of an ESP used for ignition in a real automobile engine. Investigations on laser energy parameterization of the Solderjet Bumping technique were performed in order to choose suitable working parameters that would melt the soldering bumps while still avoiding damage to the optical components. The soldering procedure was then performed and the LSP device assembled. The LSP could yield laser pulses of 0.8-ns duration, with energy between 2.40 and 4.70 mJ, thus being useful for LI of both stoichiometric and lean air-fuel mixtures.

The Solderjet Bumping technique applies a localized input of thermal energy, using a laser pulse to reflow, melt, and place soft solder alloys onto different materials [Fig. 1(a)]. In this way, brittle materials such as those used for lenses can be soldered to the device housing without damaging the components. However, this process requires the obtaining of metallic wettable surfaces over the optical components. Such metallic interfaces can be obtained via physical vapor deposition (PVD) [Fig. 1(b)].

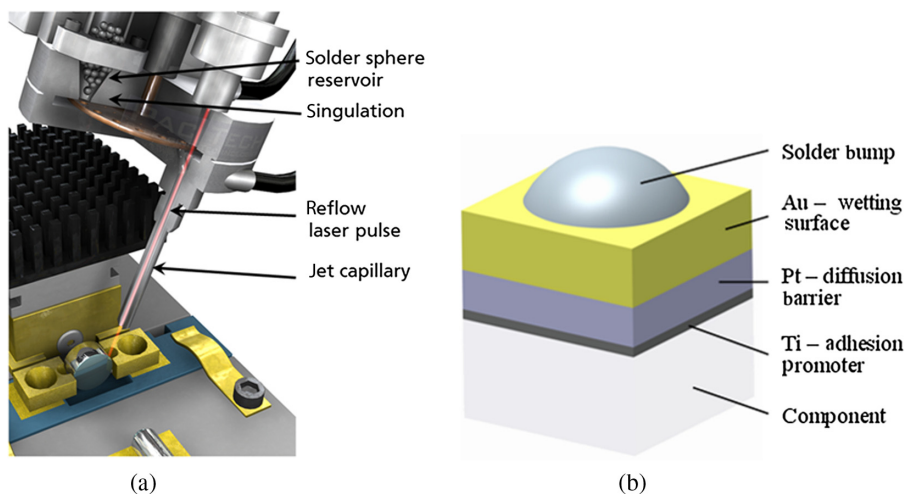


Fig. 1 (a) Schematic of Solderjet Bumping bondhead. (b) Example of three applied layers (Ti/Pt/Au) creating a wettable surface over components to be joined.^{16,21}

2 Device Design

2.1 Mechanical Design

The mechanical design replicates with a monolithic housing ($\sim\varnothing 20 \times 70$ mm) the size and geometry of a common ESP; thus it can be fastened to a combustion chamber by an M14 \times 1.25 mm thread. The LSP is separated from the combustion chamber by a sapphire window ($\varnothing 5 \times 2$ mm) soldered onto the tip of the housing body. The internal optical components, i.e., the lenses and the Nd:YAG/Cr⁴⁺:YAG active media, were axially preloaded and pressed between the housing front end and the end flange. The optical fiber delivering the pump beam was screwed onto this flange [Fig. 2(a)].

In order to solder the optical components, they have been locally metalized (Ti/Pt/Au layers were applied by PVD) to allow soldering wettability at the lens edges, while also ensuring suitable dimensions of the clear aperture for the laser beam transmission. Later, the lenses were soldered to independent stainless steel frames [Fig. 2(b)]. In the eventual case of lens tilt resulting from the assembling procedure, the stainless-steel-independent bodies could be radially and axially readjusted (with accuracy of better than $2 \mu\text{m}$) by an alignment turning procedure.²² Pump-beam absorption creates a rising temperature, so the Nd:YAG/Cr⁴⁺:YAG laser medium was placed inside a copper heat-sink for better heat dissipation.

Finite-element-method (FEM) simulations were performed to ensure that the assemblies could withstand the environmental conditions of a working engine. Figure 3 shows the initial thermal modeling with a temperature load of $\Delta T = 200$ K. A linear elongation of the main body of $163 \mu\text{m}$ from the fixation point (which was the M14 \times 1.25 mm thread screwed into the combustion chamber body) was evaluated; however, this was not an issue for the flexible body of the optical fiber. Modal analysis was performed on three axes (X, Y, and Z), at 1993, 1995, 3914, and 3917 Hz. No irreversible deformation of the components was observed.

2.2 Optical Design

Optical simulations were performed using the Zemax optical design software to ensure that the LI design based on a

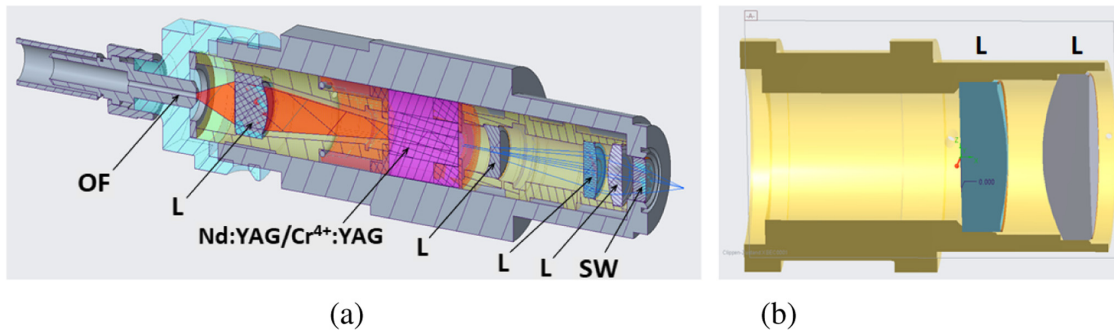


Fig. 2 (a) Optical components and the Nd:YAG/Cr⁴⁺:YAG medium inserted into the stainless-steel main body. OF, optical fiber; L, lens; SW, sapphire window. (b) An independent stainless-steel body with two soldered lenses.

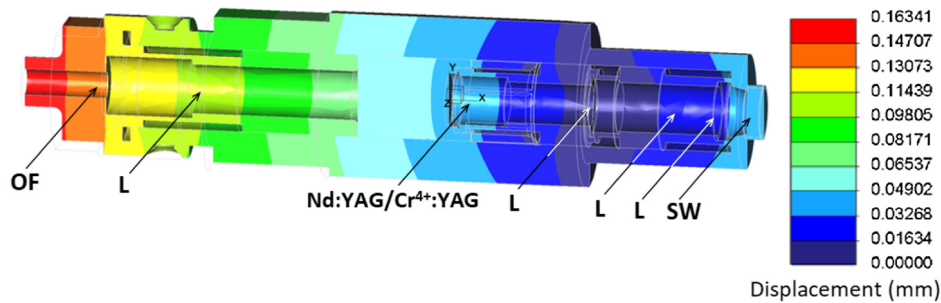


Fig. 3 Example of initial thermal FEM analysis results. OF, optical fiber; L, lens; SW, sapphire window.

soldering procedure can provide laser pulses comparable to an LSP assembled via an adhesive technique.¹³ The designs were divided into two systems; the pump line and the focusing line. The pump line was used to focus the laser beam (wavelength of 807 nm) from the optical fiber (600 μm fiber core diameter with NA = 0.22) into the Nd:YAG/Cr⁴⁺:YAG active medium. In our case, the laser medium was a composite Nd:YAG/Cr⁴⁺:YAG ceramic (Ø5 × 11 mm) from Baikowski Co., Japan. The focusing line was designed to bring the laser beam to the point where the air breakdown phenomenon takes place, similar to the position of the electrical discharge in an ESP.

Figure 4 shows a diagram in which the pump beam was focused to a radius of 1.5 mm at a position 6 mm inside the Nd:YAG/Cr⁴⁺:YAG ceramic. For the focusing line, assuming a laser waist ω_0 (1/e² radius) of 600 μm at the exit face of the laser material, the paraxial Gaussian beam analysis resulted in a diffraction-limited 14 μm 1/e² spot size at the focus point.

3 Assembly Process

3.1 Solderjet Bumping Laser Energy Parameterization

The main advantage of soldering brittle materials with the Solderjet Bumping technique is the possibility of precisely adjusting the laser melting energy to avoid damage to glass or crystal components. In the current case of study, the lenses were manufactured from a wide range of materials (ECO-550 Glass, D-ZLaF52LA, TAC4, and N-SF11). To make sure that each lens and the sapphire window could be properly soldered to the stainless steel frame using different soft solder alloys (96.5Sn3Ag0.5Cu and 80Au20Sn), the appropriate reflow and melting energy for Solderjet Bumping was determined. For this purpose, an experiment with 25 different energy points varying the solderjet laser pulse duration (in ms) and laser current (in mA) was performed. The optical materials were metalized beforehand with Ti/Pt/Au layers via PVD techniques.

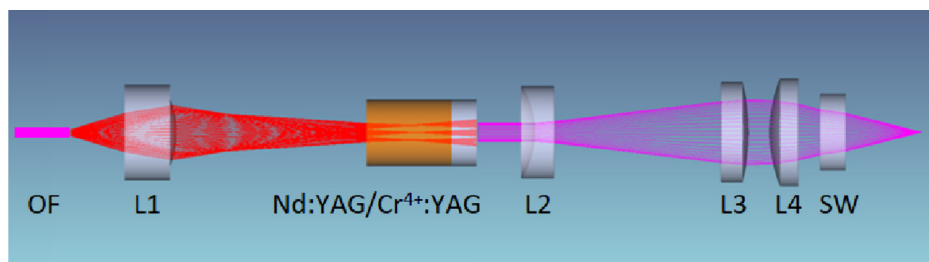


Fig. 4 Schematic of the Zemax modeling for the pump line (L1), the Nd:YAG/Cr⁴⁺:YAG medium and the focusing line (L2, L3, and L4).

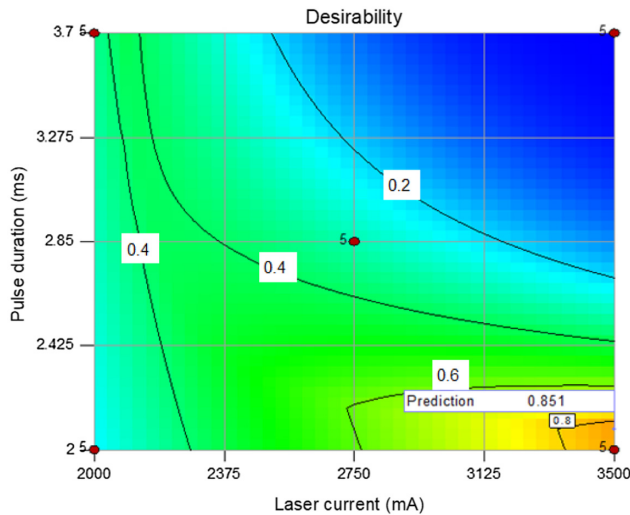


Fig. 5 Desirability results to solder N-SF11 to stainless steel. Desirable energy obtained by varying laser current (mA) and laser pulse (ms).

After performing these 25 bump processes of different energies to the optical materials, we studied the material damage and bump reflowed diameter for each sample.^{16,21} The damage was visually observed through a microscope. The assessment was done mainly to ensure any cracks or abrasion produced by the thermomechanical stress of soldering were avoided. The reflowed melted diameter, also visually analyzed, was studied to ensure correct alloy wettability and adhesion on the substrate materials.²³ As an example, Fig. 5 presents the required energy to reflow the 96.5Sn3Ag0.5Cu (SAC305) alloy to bond stainless steel and N-SF11 materials; this represents a Solderjet Bumping parameterization of 3500 mA and 2.1 ms (about 43 mJ pulse energy). The results determined for all materials are summarized in Table 1. Once the required energy and consequent Solderjet Bumping parameterization were obtained to properly solder each optical material to stainless steel, the lenses, and window could be assembled for the spark plug bodies [as sketched in Fig. 2(b)].

3.2 Optical Components Soldering Procedure

Before assembling the optical components, the lenses and the sapphire window had been locally metalized with Ti/Pt/Au layers in order to create wettability and a solderable surface on the edges. The metallization rim covered up to around 300 μm from each component edge; this ensured an adequate optical aperture to allow the laser beam to

traverse the components and provided enough area to apply soldering bumps of 200 μm diameter. The stainless steel frames and the main spark plug body had, in contrast, been fully metalized with Ti/Pt/Au layers, since this does not affect the optical system (but, again, it ensures the alloy wettability).¹⁶

The pump lens (composed of D-ZLaF52LA) and the focusing line lenses (made of ECO-550 Glass, TAC4, and N-SF11) were soldered using six droplets of 200- μm diameter SAC305 alloy equally spaced around the perimeter [Fig. 6(a)]; a close-up view of a bump used to fix the lens edge to the stainless-steel body of the LSP is shown in Fig. 6(b). The energy used in each case was according to the data given in Table 1. The required amount of soldering alloy guarantees the necessary robustness to withstand modal environments.²¹

The sapphire window was also soldered to the stainless steel main body [Fig. 7(a)], using a continuously applied soldering rim of approximately 300 droplets of 200 μm diameter 80Au20Sn (AuSn) alloy [Fig. 7(b)]. This continuous alloy line was created to prevent fuel from being injected into the LSP device.

Finally, all the independent components (lenses soldered inside the stainless steel frames and the Nd:YAG/Cr⁴⁺:YAG medium placed in the copper frame) were inserted in the LI spark plug main body and then pushed and pressed by a flange to which the optical fiber was coupled.

4 Results

The experimental conditions were comparable to those used by Pavel et al.¹³ Thus, the laser medium was a composite Nd:YAG/Cr⁴⁺:YAG ceramic/polycrystalline structure (Baikowski Co., Japan), consisting of a 1.0-at. %, 8-mm long Nd:YAG, which was diffusion bonded to a 3-mm long Cr⁴⁺:YAG SA ceramic with initial transmission $T_0 = 0.40$. A monolithic resonator was obtained by coating the high reflectivity mirror (reflectivity, $R > 0.999$ at 1.06- μm lasing wavelength) on the Nd:YAG side facing the pump line; this Nd:YAG side was also coated for high transmission ($T > 0.98$) at the pump wavelength of 807 nm. The OCM was directly coated on the free surface of the Cr⁴⁺:YAG. The pumping at 807 nm was by fiber-coupled diode lasers (JOLD-120-QPXF-2P, Jenoptik, Germany) which were operated in quasicontinuous-wave mode at a repetition rate of up to 100 Hz; the pump pulse duration was 250 μs .

Such an LSP device can be installed on a real automobile engine, which usually operates with a stoichiometric $\lambda \sim 1$ air-fuel ratio.¹³ On the other hand, LI is very promising

Table 1 Final results for soldering different optical materials to the stainless steel bodies.

Optical material	Substrate	Alloy	Laser pulse (ms)	Laser current (mA)	Energy (mJ)
Sapphire	Stainless steel	80Au20Sn	3.7	3500	~58
ECO-550 glass	Stainless steel	SAC305	3.7	2060	~41
D-ZLaF52LA	Stainless steel	SAC305	3.7	2170	~42
TAC4	Stainless steel	SAC305	2.1	3500	~43
N-SF11	Stainless steel	SAC305	2.1	3500	~43

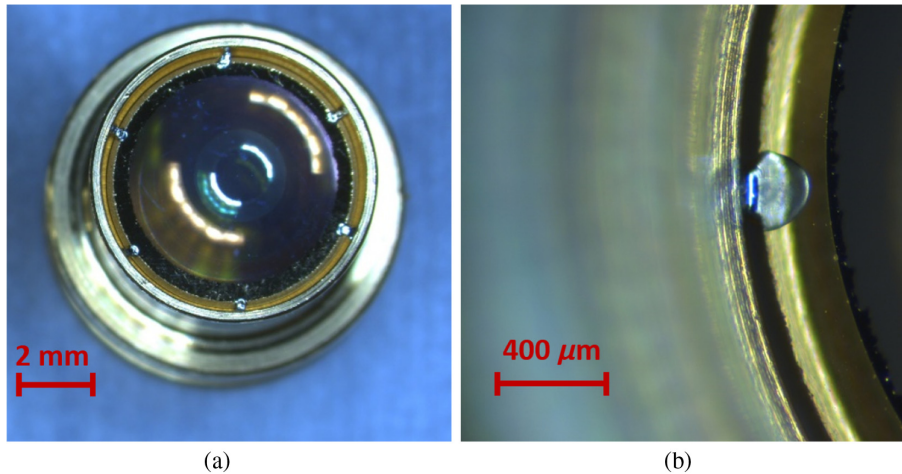


Fig. 6 (a) A soldered lens with six SAC305 bumps (200 μm diameter), as in Fig. 2(b). (b) Detail of an applied bump between the lens edge and the stainless-steel mount.

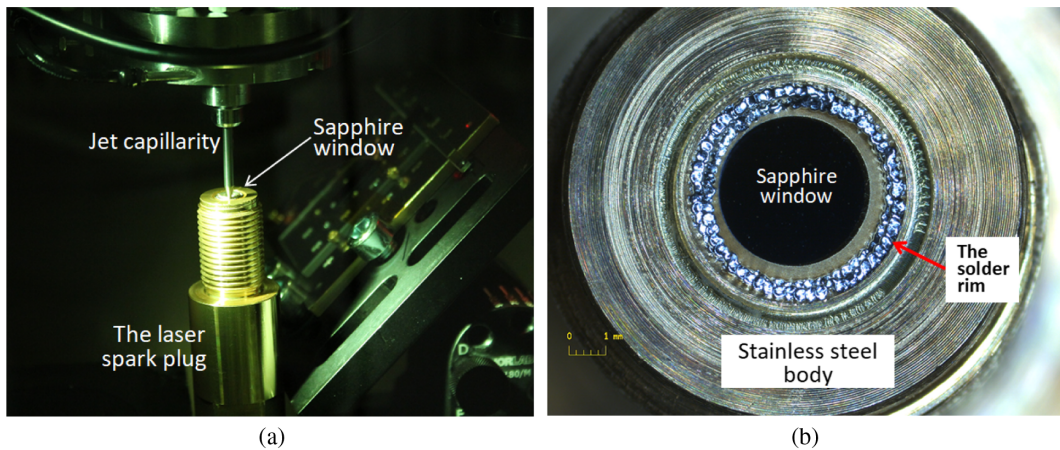


Fig. 7 (a) Solderjet Bumping process: applying bumps on the sapphire window circumference. (b) Detail of continuous bumps applied between the sapphire window edge and the stainless-steel mount.

when the engine is run with lean, $\lambda > 1$ air–fuel mixtures.²⁴ To satisfy such different working conditions, the LSP must be able to deliver trains of laser pulses, as well as pulses of variable energy. To achieve this goal, in our design, the pump unit, the Nd:YAG/Cr⁴⁺:YAG stage, and the focusing line were made as independent, fixed units, whereas the distance between the optical fiber and the pump lens (of 6-mm-focal length) was varied.

Figure 8 presents the LSP performances versus distance d (the distance between the optical fiber and the pump lens). Laser pulses with energy ranging from 2.40 to 4.70 mJ were obtained by decreasing d from 7.5 to 5.9 mm. It should be noted that the pump pulse energy E_{pump} was in the range of 40 to 42.5 mJ. These results are comparable to those reported in our previous work.¹³ It is worth noting that this new design allows for a quick and simple change of the laser pulse energy, which could be beneficial for LI of air–fuel mixtures in variable conditions, but also for other specific industrial applications. Some LSPs assembled in this work are shown in Fig. 9(a). The air breakdown phenomenon induced by an LSP with a pulse energy $E_p = 2.80$ mJ is presented in

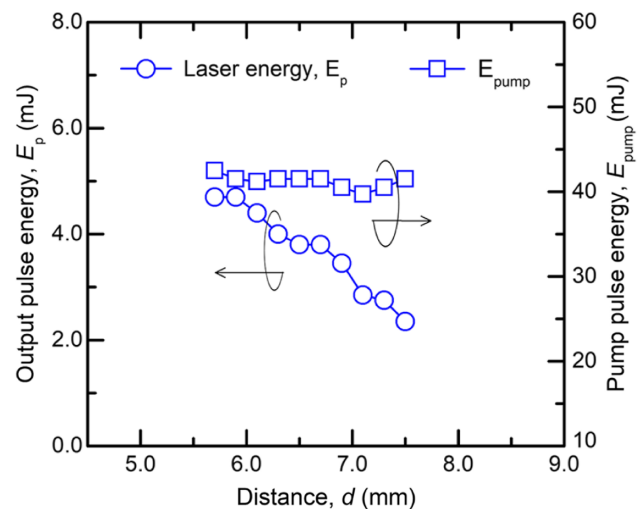


Fig. 8 Laser pulse energy E_p and corresponding pump pulse energy, E_{pump} versus distance d , between the optical fiber and the pump lens.

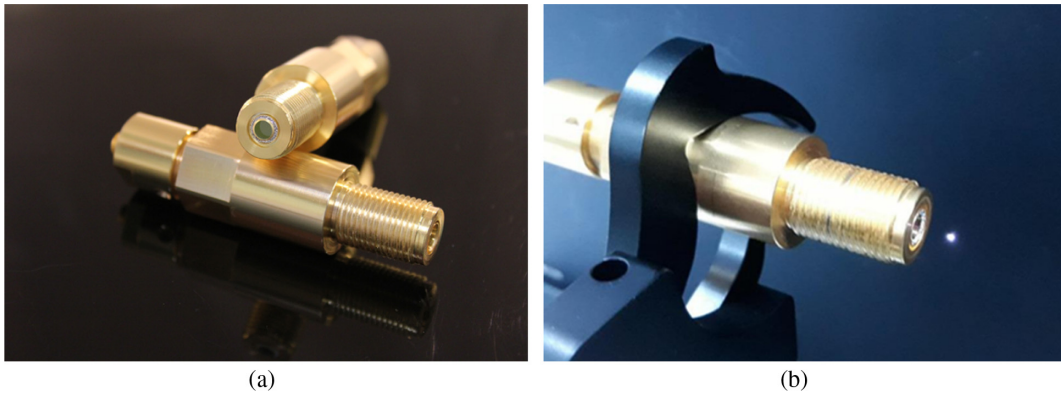


Fig. 9 (a) Some assembled golden laser spark plugs are shown. (b) Air breakdown produced by the 2.80-mJ laser pulse.

Fig. 9(b). Testing of the new LSP on a real automobile engine will be considered in future experiments.

5 Conclusions

In order to guarantee higher device robustness,¹⁸ an LI spark-plug device has been assembled using the Solderjet Bumping technique. The resulting LSP shows similar pulse performances to previous devices reported whose optical components were fixed using adhesive. Preliminary experiments proved that soldered sapphire windows resisted up to 200 atm pressure (the maximum available in our experimental conditions). Further investigations, as well as mounting on a real automobile engine, are necessary to fully verify the LSP functionality. On the other hand, the Solderjet Bumping technique applied on the current LSP design may be a solution for carrying out integrated and automatized manufacturing processes, which could lead to an affordable production price. Moreover, LI is now undergoing its first steps to be integrated in rocket launchers and satellite thrusters.^{25,26} It would be difficult to integrate and space qualify such devices using standard epoxies due to the outgassing behaviors in vacuums. Solderjet Bumping could here provide a feasible solution, since it uses inorganic bonding materials and a technology already qualified for a space mission.²⁷

As a final remark, since the device body and lenses have been metalized with Au layers, the LSP laser spark plug had an unusual golden color; therefore, we have named the LSP device the golden laser spark plug.

Acknowledgments

The authors acknowledge support from the European Union's Horizon 2020 Research and Innovation Program under Grant Agreement No. 691688 LASIG-TWIN and partial financing from project 157/2017, PN-III-P4-ID-PCE-2016-0332, Ministry of Research and Innovation, Romania, CNCS-UEFISCDI. Authors thank other Fraunhofer IOF members, which helped during trainings in the framework of the LASIG-TWIN project, especially to Marcel Hornaff, Maria Kepper, and Sai Priya Somvanshi, finally, to Dr. Rossá Gerard Mac Ciarnáin from Physics Proof and Aoife Brady. Disclosures: The authors have no relevant financial interests in the manuscript and no other potential conflicts of interest to disclose.

References

1. P. Ronney, "Laser versus conventional ignition of flames," *Opt. Eng.* **33**(2), 510–521 (1994).
2. J. Tauer, H. Kofler, and E. Wintner, "Laser-initiated ignition," *Laser Photonics Rev.* **4**(1), 99–122 (2010).
3. M. H. Morsy, "Review and recent developments of laser ignition for internal combustion engines applications," *Renew. Sust. Energy Rev.* **16**(7), 4849–4875 (2012).
4. N. Pavel et al., "Laser ignition: spark plug development and application in reciprocating engines," *Prog. Quantum Electron.* **58**, 1–32 (2018).
5. J. D. Dale, P. R. Smy, and R. M. Clementsi, "Laser ignited internal combustion engine: an experimental study," *SAE Int.* **87-A**, 780329 (1978).
6. J. Mullett et al., "Multi-cylinder laser and spark ignition in an IC gasoline automotive engine: a comparative study," *SAE Int.* **SP-2187**, 0470 (2008).
7. M. Weinrotter, H. Kopecek, and E. Wintner, "Laser ignition of engines," *Laser Phys.* **15**(7), 947–953 (2005).
8. H. Kofler et al., "An innovative solid-state laser for engine ignition," *Laser Phys. Lett.* **4**(4), 322–327 (2007).
9. G. Kroupa, G. Franz, and E. Winkelhofer, "Novel miniaturized high-energy Nd:YAG laser for spark ignition in internal combustion engines," *Opt. Eng.* **48**(1), 014202 (2009).
10. M. Tsunekane et al., "High peak power, passively Q-switched micro-laser for ignition of engines," *IEEE J. Quantum Electron.* **46**(2), 277–284 (2010).
11. N. Pavel, M. Tsunekane, and T. Taira, "Composite, all-ceramics, high-peak power Nd:YAG/Cr⁴⁺:YAG monolithic micro-laser with multiple-beam output for engine ignition," *Opt. Express* **19**(10), 9378–9384 (2011).
12. T. Taira et al., "World first laser ignited gasoline engine vehicle," in *1st Laser Ignition Conf. (LIC13)*, Yokohama, Japan, Vol. 1, p. LIC3–1 (2013).
13. N. Pavel et al., "Ignition of an automobile engine by high-peak power Nd:YAG/Cr⁴⁺:YAG laser-spark devices," *Opt. Express* **23**(26), 33028–33037 (2015).
14. N. Pavel et al., "Laser ignition of a gasoline engine automobile," in *Laser Ignition Conf. 2017*, OSA Technical Digest (online) Optical Society of America, Vol. 5, p. LWA4.3 (2017).
15. M. Biruduganti et al., "Performance evaluation of a DENSO developed micro-laser ignition system on a natural gas research engine," in *Laser Ignition Conf.*, OSA Technical Digest (online) (Optical Society of America), Vol. 3, p. T5A.4 (2015).
16. E. Beckert et al., "Solder jetting: a versatile packaging and assembly technology for hybrid photonics and optoelectronic systems," in *Proc. IMAPS 42nd Int. Symp. Microelectron.*, California, Vol. 42, p. 406 (2009).
17. P. Ribes et al., "Solderjet bumping technique used to manufacture a compact and robust green solid-state laser," *Proc. SPIE* **9520**, 952009 (2015).
18. P. Ribes-Pleguezuelo et al., "Assembly processes comparison for a miniaturized laser used for the ExoMars European Space Agency Mission," *Opt. Eng.* **55**, 116107 (2016).
19. P. Ribes-Pleguezuelo et al., "Method to simulate and analyse induced stresses for laser crystal packaging technologies," *Opt. Express* **25**(6), 5927–5940 (2017).
20. P. Ribes-Pleguezuelo et al., "Study of a laser packaging technique simulated with ANSYS and VirtualLab Fusion software," in *5th Laser Ignition Conf.*, Bucharest, Romania, OSA Technical Digest (online) (Optical Society of America), Vol. 5, p. LWA2.4 (2017).
21. P. Ribes-Pleguezuelo et al., "Lithiumniobate die assembled by a low-stress soldering technique-method to fasten a surface acoustic wave

- sensor," in *6th Int. Conf. Photonics, Opt. and Laser Technol. (PHOTOPTICS)*, Madeira, Portugal, Vol. 6, pp. 91–97 (2018).
22. M. Beier et al., "Lens centering of aspheres for high-quality optics," *Adv. Opt. Technol.* **1**(6), 441–446 (2012).
 23. M. Mäusezahl et al., "Mechanical properties of laser-jetted SAC305 solder on coated optical surfaces," *Phys. Procedia* **83**, 532–539 (2016).
 24. A. Birtas et al., "On the possibility to improve petrol engine operation by laser ignition," *Energy Procedia* **157**, 1022–1028 (2019).
 25. C. Manfletti and G. Kroupa, "Laser ignition of a cryogenic thruster using a miniaturised Nd:YAG laser," *Opt. Express* **21**(56), A1126–A113 (2013).
 26. S. Soller, N. Rackermann, and G. Kroupa, "Laser ignition application to cryogenic propellant rocket thrust chambers," in *Laser Ignition Conf. 2017, OSA Technical Digest (online)*, Vol. 5, p. LFA4.3 (2017).
 27. P. Ribes-Pleguezuelo et al., "Insights of the qualified ExoMars laser and mechanical considerations of its assembly process," *MDPI Instrum.* **3**(2), 25 (2019).

Pol Ribes-Pleguezuelo received his diploma degree in physics from the University of Barcelona, Spain, in 2008. From 2010 to 2013, he worked as a researcher in the design, manufacturing, and marketing of low/high power diodes and advanced solid-state lasers at Monocrom SL, Spain. Since 2013, he has been working at the Fraunhofer Institute of Applied Optics and Precision Engineering IOF, Jena. In 2018, he received his PhD from the Friedrich-Schiller-University Jena, Germany.

Nicolai Pavel graduated from the Faculty of Physics, Bucharest University in 1990. He received his PhD in optics, spectroscopy, and lasers from Institute of Atomic Physics, Bucharest, Romania, in 1997, and in 2013, he habilitated. He has been with the National Institute for Laser, Plasma, and Radiation Physics, Magurele, Romania, since 1990. His research interests include diode-pumped solid-state laser, waveguide lasers realized by direct writing with a femtosecond-laser beam, high-peak power lasers for laser ignition.

Erik Beckert received the diploma degree in precision mechanics and his PhD in optoelectronics system integration from the Technical University Ilmenau, Germany, in 1997 and 2005, respectively. In 2001, he joined the Fraunhofer Institute for Applied Optics and Precision Engineering IOF, Jena, Germany. Since 2005, he has been the head of the microassembly and system integration group at Fraunhofer IOF. His research interests include, i.e., assembly and integration of optical and optomechanical systems and soldering technology developments.

Christoph Damm received his diploma degree in high precision instrument technology and construction from the Applied Science University of Jena, Germany, in 1984. From 1984 to 1992 worked as an engineer for the research and construction of precision instruments for the Friedrich-Schiller-University Jena. Since 1992, he has been working in the mechanical simulations and designs for the Fraunhofer Institute of Applied Optics and Precision Engineering IOF, Jena, Germany.

Axel Bodemann received his diploma degree in physics from Friedrich-Schiller-University Jena, Germany, in 1992. From 1998 to 2011, he was working for Carl Zeiss AG, microcopy as well as for the research and technology, Optical Design Department. Since 2012, he has been working at the Fraunhofer Institute of Applied Optics and Precision Engineering IOF, Jena, Germany. His research

interests include design and optimization of micro-optical systems for imaging and illumination applications.

Oana-Valeria Grigore graduated in medical physics in 2008 and obtained a master's degree in physics, in 2010, from Faculty of Physics, University of Bucharest, Romania. Currently, she is a PhD student at the same faculty. Since 2007, she has been working at the National Institute for Laser, Plasma and Radiation Physics, Magurele, Romania. Her research regards solid-state laser physics, interaction of high-power laser beams with matter and applications of THz radiation.

Gabriela Croitoru received her diploma degree and master's degree in medical physics from the Faculty of Physics, University of Bucharest, Romania, in 2008 and 2010, respectively. She is currently employed as a scientific researcher at the National Institute for Lasers, Plasma and Radiation Physics, Magurele, Romania. Her research interests include realization of waveguide lasers by direct writing technique with a femtosecond-laser beam, diode-pumped solid-state lasers, and short pulse generation.

Catalina-Alice Brandus received her diploma in biophysics and her master's degree in biophysics and medical physics, electronics and metrology, in 2008 and 2010, respectively, at the Faculty of Physics, University of Bucharest, Romania. From January 2010, she works at Solid-State Quantum Electronics Laboratory of the National Institute for Laser, Plasma, and Radiation Physics, Magurele, Romania. Her current research interest is focused on diode-pumped solid-state lasers operating in free generation and ultra-short pulse regimes.

Nicolai-Tiberius Vasile received his diploma degree in engineering physics from Faculty of Physics, the University of Bucharest, Romania, in 2009. In November 2016, he was granted by the same university a PhD in physics after successfully defending his thesis. Since 2010, he has been working as a researcher at the National Institute for Laser Plasma and Radiation Physics, Magurele. His research interests include a range of computational imaging techniques, such as image super-resolution, multiplexed imaging, and coded-aperture imaging.

Ramona Eberhardt received her diploma and PhD degrees in chemistry from Friedrich-Schiller-University Jena, Germany, in 1982 and 1987, respectively. From 1992 to 2004, she was a group manager of the microassembly group at the Fraunhofer Institute for Applied Optics and Precision Engineering IOF, Jena. Since 2005, she has been the head of the Department of Precision Engineering at Fraunhofer IOF. Her experiences include precision fixation technologies such as soldering and adhesive bonding, material sciences, and packaging of optomechanical systems.

Andreas Tünnermann received his diploma and PhD degrees in physics from the University of Hannover, Germany, in 1988 and 1992, respectively. In 1997, he habilitated. He was head of the Development Department at the Laser Zentrum Hannover from 1992 to 1997. In 1998, he joined the Friedrich-Schiller-University Jena, Germany, as a professor and a director of the Institute of Applied Physics. In 2003, he additionally became director of the Fraunhofer Institute for Applied Optics and Precision Engineering IOF, Jena.